Magnetic-coherence-length scaling in metallic multilayers

R. T. W. Koperdraad and A. Lodder

Faculteit Natuurkunde en Sterrenkunde, Vrije Universiteit, De Boelelaan 1081, 1081 HV Amsterdam, The Netherlands

An improved description of the critical properties of metallic multilayers is obtained by introducing the concept of a scaled magnetic coherence length in the Takahashi-Tachiki theory. By that, the absolute magnitude of the upper critical fields and the position of the dimensional crossover are uncoupled and become independent quantities. Much better phase diagrams can be obtained by using this scaling procedure. Although this concept is inspired by the character of disagreement between the theory without scaling and experiment, the procedure lacks an external justification. The fact that it works might serve as an indication how the Takahashi-Tachiki theory has to be modified in order to give a realistic quantitative description of upper critical fields in real metallic multilayers. The theory is applied to the V/Cu, V/Ag, Nb/Cu, and Nb/Ag systems. [S0163-1829(96)06425-9]

I. INTRODUCTION

The state of the art of thin-film technology has allowed for the fabrication of high-quality multilayer samples. That gave experimentalists the opportunity to come to a detailed analysis of the upper critical fields of these systems. Since Schuller and co-workers finished their series of experiments,[1–4] a wealth of information is available for the Nb/Cu multilayer system. Similarly, Kanoda *et al.*[5,6] did elaborate experiments on V/Ag multilayers, whereas Broussard and Geballe[7,8] studied Nb/Ta extensively. It is the quantitative description of these experiments that now seems to be the most important task.

Recently, we have given a critical review[9] of theoretical studies that dealt with the proximity effect. It was concluded that no thorough comparison of theory and experiment existed that considers absolute magnitudes of both parallel and perpendicular upper critical fields in multilayers of various layer thicknesses. We made an attempt[9,10] to such a comparison for two related systems: V/Ag and Nb/Cu. The exact solutions were calculated of the well-known Takahashi-Tachiki equations,[11] which constitute the most advanced proximity-effect theory currently available. However, a good matching of calculations with experimental data could not always be achieved. Particularly, there was a disagreement in the position of the dimensional crossover in the parallel upper critical field. This position is mainly determined by the magnetic coherence length.

The present paper provides a new look at the solutions of the Takahashi-Tachiki equations by introducing the additional concept of magnetic-coherence-length scaling. By that, the absolute magnitude of the upper critical fields and the position of the dimensional crossover become independent quantities. It will be shown that by this scaling procedure better phase diagrams can be obtained. Section II gives a short exposition of the original Takahashi-Tachiki formalism. Section III recalls the earlier results of our efforts and points out the basic problems we encountered in earlier studies. It prepares the idea of magnetic-coherence-length scaling, which is introduced in Sec. IV. In Secs. V and VI, the idea of scaling is applied to the V/Ag and Nb/Cu systems,

respectively. Section VII treats the related systems V/Cu (Ref. 12) and Nb/Ag.[13] Section VIII summarizes the conclusions.

II. THEORY

The starting point of the Takahashi-Tachiki theory[11,14] is Gorkov's linearized integral equation for the pair potential[15]

$$\Delta(\mathbf{r}) = \int K(\mathbf{r},\mathbf{r}')\Delta(\mathbf{r}')d^3r'. \tag{1}$$

The kernel $K(\mathbf{r},\mathbf{r}')$ can be expanded as

$$K(\mathbf{r},\mathbf{r}') = V(\mathbf{r})kT\sum_{\omega} Q_{\omega}(\mathbf{r},\mathbf{r}'), \tag{2}$$

which contains a position-dependent BCS electron-electron interaction coupling constant $V(\mathbf{r})$ and a summation over discrete frequencies $\omega = (2n+1)\pi kT$. The summation is restricted to frequencies $|\omega| \leq \omega_D$, ω_D being the Debye frequency. According to Takahashi and Tachiki, $Q_{\omega}(\mathbf{r},\mathbf{r}')$ can be derived from a set of coupled differential equations, including diamagnetic and paramagnetic effects. Auvil, Ketterson, and Song[16] generalized these equations to include also magnetic impurity scattering and spin-orbit scattering. For nonmagnetic dirty type-II superconductors, however, these reduce to the single Green's-function-like differential equation

$$[2|\omega| + L(\boldsymbol{\nabla})]Q_{\omega}(\mathbf{r},\mathbf{r}') = 2\pi N(\mathbf{r})\delta(\mathbf{r}-\mathbf{r}'), \tag{3}$$

where $N(\mathbf{r})$ is the position-dependent density of states at the Fermi energy. The differential operator $L(\boldsymbol{\nabla})$ is given by

$$L(\boldsymbol{\nabla}) \equiv -\hbar D(\mathbf{r})\left(\boldsymbol{\nabla} - \frac{2ie\mathbf{A}(\mathbf{r})}{\hbar c}\right)^2, \tag{4}$$

$D(\mathbf{r})$ being the position-dependent electronic diffusion constant and $\mathbf{A}(\mathbf{r})$ the vector potential of the applied magnetic field. For multilayers, the three functions $N(\mathbf{r})$, $V(\mathbf{r})$, and $D(\mathbf{r})$ are assumed to be constant within a single material, making discontinuous jumps at the interfaces.

We now define the pair function $F(\mathbf{r}) \equiv \Delta(\mathbf{r})/V(\mathbf{r})$. It was the idea of Takahashi and Tachiki to solve Eqs. (1) and (3) by using an expansion of $Q_\omega(\mathbf{r},\mathbf{r}')$ and $F(\mathbf{r})$ in terms of the eigenfunctions $\psi_\lambda(\mathbf{r})$ of the operator $L(\boldsymbol{\nabla})$, with corresponding eigenvalues ϵ_λ:

$$F(\mathbf{r}) = \sum_\lambda c_\lambda \psi_\lambda(\mathbf{r}) \tag{5a}$$

and

$$Q_\omega(\mathbf{r},\mathbf{r}') = \sum_{\lambda,\lambda'} a_{\lambda,\lambda'}^\omega \psi_{\lambda'}^*(\mathbf{r}')\psi_\lambda(\mathbf{r}). \tag{5b}$$

The eigenfunctions have to obey the de Gennes boundary conditions[17] demanding the continuity of $\psi_\lambda(\mathbf{r})/N(\mathbf{r})$ and $D(\mathbf{r})[\boldsymbol{\nabla} - 2ie\mathbf{A}(\mathbf{r})/\hbar c]\psi_\lambda(\mathbf{r})$. The orthogonality and closure properties read as

$$\int d^3r\, \psi_\lambda^*(\mathbf{r})\frac{1}{N(\mathbf{r})}\psi_{\lambda'}(\mathbf{r}) = \delta_{\lambda\lambda'} \tag{6}$$

and

$$\sum_\lambda \psi_\lambda^*(\mathbf{r})\psi_\lambda(\mathbf{r}') = N(\mathbf{r})\delta(\mathbf{r}-\mathbf{r}'), \tag{7}$$

reflecting the discontinuous nature of $N(\mathbf{r})$. Substitution of (5) in Eqs. (1) and (3) finally leads to a matrix equation for the coefficients c_λ:

$$c_\lambda = \sum_{\lambda'}\left(2\pi kT\sum_\omega \frac{1}{2|\omega|+\epsilon_\lambda}\right)V_{\lambda\lambda'}c_{\lambda'}, \tag{8}$$

where $V_{\lambda\lambda'}$ is the matrix element $\langle\psi_\lambda|V|\psi_{\lambda'}\rangle$. When the secular equation

$$\det\left|\delta_{\lambda\lambda'} - 2\pi kT\sum_\omega \frac{1}{2|\omega|+\epsilon_\lambda}V_{\lambda\lambda'}\right| = 0 \tag{9}$$

is satisfied, there are nontrivial solutions for the coefficients c_λ and consequently for the pair function $F(\mathbf{r})$. The highest temperature for which such a solution exists is the field-dependent critical temperature. The present authors showed[14] that the frequency summation appearing in (9) can be evaluated exactly in terms of the digamma function $\Psi(x)$, using the identity

$$2\pi kT\sum_\omega \frac{1}{2|\omega|+\epsilon_\lambda} = \Psi\left(\frac{\omega_D}{2\pi kT}+\frac{\epsilon_\lambda}{4\pi kT}+1\right)$$
$$-\Psi\left(\frac{\epsilon_\lambda}{4\pi kT}+\frac{1}{2}\right). \tag{10}$$

The behavior of Eq. (9) in the thin-layer limit is useful in understanding the origin of the two solutions of our fit procedure, to be described in Sec. III. In this limit the thicknesses d_S and d_N of the superconducting and normal layers, respectively, approach zero and the multilayer behaves as an average bulk metal. One can use the diagonal approximation,[14] which implies that in expansions (5) only the ground-state wave function is used. Equation (9) then simplifies to

$$\Psi\left(\frac{\omega_D}{2\pi kT}+\frac{\epsilon_G}{4\pi kT}+1\right)-\Psi\left(\frac{\epsilon_G}{4\pi kT}+\frac{1}{2}\right) = \frac{1}{V_{GG}}, \tag{11}$$

where the index G refers to the ground state. The expression for the ground-state eigenvalues depends on the direction of the magnetic field. They can be shown[14] to read as

$$\epsilon_G^\perp = \frac{\hbar}{\xi^2}\frac{\langle ND\rangle}{\langle N\rangle} \tag{12}$$

for perpendicular magnetic fields and

$$\epsilon_G^\parallel = \frac{\hbar}{\xi^2}\frac{1}{\langle N\rangle}\sqrt{\langle ND\rangle\left\langle\frac{1}{ND}\right\rangle^{-1}} \tag{13}$$

for parallel magnetic fields, where ξ is the magnetic or Ginzburg-Landau coherence length, given by

$$\xi = \sqrt{\frac{\hbar c}{2eH}}. \tag{14}$$

The angular brackets denote the spatial average of the bracketed quantities, e.g., $\langle N\rangle \equiv (N_S d_S + N_N d_N)/(d_S + d_N)$. The expression for the ground-state matrix element V_{GG} is independent of the field direction and reads as

$$V_{GG} = \frac{\langle N^2 V\rangle}{\langle N\rangle}. \tag{15}$$

III. EARLIER RESULTS REVISITED

In two previous papers[9,10] on upper critical fields in metallic multilayers, a fit procedure was adopted to find out about the ability of the theory to reproduce the data. To that end three material parameters were used as free quantities. These were the diffusion coefficients of both metals and the density of states of the superconductor, D_S, D_N, and N_S, respectively. We recall that there are eight material parameters that characterize a multilayer: the density of states at the Fermi level N, the BCS coupling constant V, the diffusion coefficient D, and the Debye temperature Θ_D for each of the two metals. Since the theory does not account for the two metals having different Debye temperatures, an average value must be used for this quantity. It was possible to make a reasonable choice for the parameters N_N, V_N, and V_S, which were assumed to be layer-thickness independent. The free parameters were used to fit the experimental multilayer T_c and the critical fields $H_{c2,\perp}(T)$ and $H_{c2,\parallel}(T)$ for a specific temperature T. Consequently, they were allowed to vary from system to system and were expected to show a dependence on the thickness of the layers. All other material parameters were assumed to be layer-thickness independent. It was argued in Ref. 9 why this is justified.

In using this fit procedure, it turned out that there are two possible outcomes for each phase diagram. A feeling for the origin of this is obtained by examining the thin-layer limit. In this limit an expression for the anisotropy, defined as the ratio of the parallel and perpendicular upper critical fields at a certain temperature, can be derived analytically, using Eqs. (11) – (15). Given the temperature, Eq. (11) determines the ground-state eigenvalue ϵ_G, which holds for both critical

fields, so $\epsilon_G = \epsilon_G^{\perp} = \epsilon_G^{\parallel}$. According to Eqs. (12) and (13) both $H_{c2,\perp}$ and $H_{c2,\parallel}$ are proportional to ϵ_G, although the proportionality factors differ. Therefore, in calculating $H_{c2,\parallel}/H_{c2,\perp}$, ϵ_G cancels out and the anisotropy is given by

$$\frac{H_{c2,\parallel}}{H_{c2,\perp}} = \sqrt{\langle ND \rangle \left\langle \frac{1}{ND} \right\rangle}. \qquad (16)$$

Working out the spatial averages yields

$$\frac{H_{c2,\parallel}}{H_{c2,\perp}} = \sqrt{\frac{d_A^2 + 2\gamma d_A d_B + d_B^2}{(d_A + d_B)^2}}, \qquad (17)$$

where γ is defined as

$$\gamma \equiv \frac{1}{2}\left(\frac{N_S D_S}{N_N D_N} + \frac{N_N D_N}{N_S D_S}\right). \qquad (18)$$

This quantity has a minimum value of one for $N_S D_S = N_N D_N$ and is larger otherwise. It is symmetric with respect to the interchange of the labels S and N. It is clear that an anisotropy is found as soon as $\gamma \neq 1$. In the thin-layer limit the anisotropy is temperature independent. For realistic systems, this is not true any more. The matching of the anisotropy is an important aspect of the fit procedure.

The application of the fit procedure is straightforward in the thin-layer limit. The quantities to be fitted are the multilayer T_c and $H_{c2,\parallel}(T)$ and $H_{c2,\perp}(T)$ at a certain temperature T. The free parameters are N_S, D_S, and D_N. However, while fitting, it is convenient to work with N_S, γ, and $D_{\text{eff}}^{\perp} \equiv \langle ND \rangle / \langle N \rangle$, instead of N_S, D_S, and D_N. Then each free parameter controls a distinct aspect of the phase diagram. The multilayer T_c is independent of the diffusion coefficients and consequently it completely determines N_S. The anisotropy of the upper critical field, $H_{c2,\parallel}/H_{c2,\perp}$, completely determines γ. Finally, $D_{\text{eff}}^{\perp}$ is found by fitting $H_{c2,\perp}(T)$ via Eq. (12).

From the above it is seen that the choice of free parameters leads to enough flexibility for the fit procedure to have a solution. There is, however, an ambiguity in calculating D_S and D_N from γ and $D_{\text{eff}}^{\perp}$. This is due to the fact that for a given value of γ it is impossible to decide whether $N_S D_S / N_N D_N$ is smaller or larger than one. Consequently, there are always two solutions for N_S, D_S, and D_N. If there is a solution with $N_S D_S / N_N D_N = x$, there is another with the same ratio equal to x^{-1}. In the thin-layer limit, the phase diagrams of the two solutions are indistinguishable. However, the diffusion coefficients can differ substantially.

Away from the thin-layer limit, there are still two solutions for each fit, but now the anisotropy is not a function of γ only and the solutions will have different phase diagrams. In Ref. 9 the choice is made for the solution with the larger ratio $N_S D_S / N_N D_N$, which we will call the first solution. The arguments were the following. First, for Nb/Cu, the first solution leads to fitted diffusion coefficients that are in a much better agreement with the values predicted by Banerjee et al.[1] Second, the dimensional crossovers found in the calculated phase diagrams seem to be of the same nature as the ones found experimentally, although the temperatures at which they are found are much too close to the critical temperature. It is admitted that the last argument is rather weak,
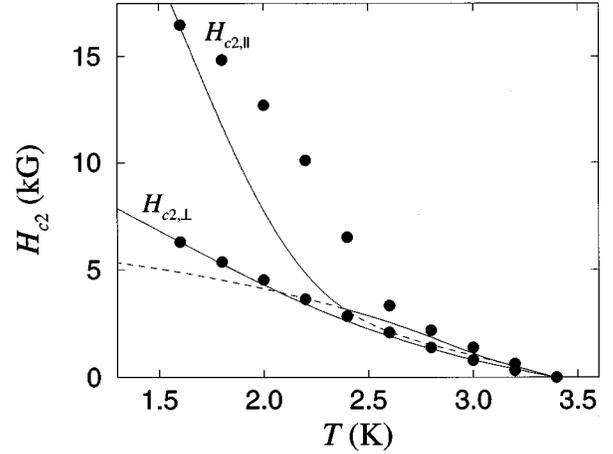
FIG. 1. Upper critical field curve of V(240 Å)/Ag(480 Å). The solid circles show the data points of Kanoda et al. (Ref. 6).

because no parameters could be found that fitted the phase diagrams of two-dimensional (2D) systems over the whole temperature range. These are the systems for which a dimensional crossover is observed in the parallel upper critical field, that is, of which the layers have intermediate thicknesses.[9]

The earlier Ref. 10 presented results according to the second solution, which is characterized by a ratio $N_S D_S / N_N D_N$ well below one. An example of such a fit is reproduced in Fig. 1. This phase diagram shows a sharp dimensional crossover in the parallel upper critical field. At this crossover the center of nucleation shifts discontinuously from one layer to the other, which yields a discontinuity in the derivative of the parallel upper critical field. This type of crossover is due to an extreme difference of the diffusion coefficients of the two metals in the multilayer. The experimental phase diagram shows no sign of the existence of such a crossover. There is a clear discrepancy between the theory and the data. Extreme fitted diffusion coefficients are the hallmark of the second solution. These values deviate substantially from the values predicted by Banerjee et al.[1] This time, the crossover temperatures are found at too low temperatures.

IV. MAGNETIC COHERENCE LENGTHS

One might wonder whether at all it is possible to obtain a reasonable phase diagram with the Takahashi-Tachiki theory. To find an answer to this question it is necessary to point out the following. The form of the dimensional crossover is largely determined by an interplay of characteristic length scales. Apart from the layer thicknesses, the theory has three of them: the Ginzburg-Landau coherence length ξ and the two BCS coherence lengths $\xi_{0,S}$ and $\xi_{0,N}$. The latter two are proportional to the square roots of the respective diffusion coefficients:

$$\xi_0(\mathbf{r}) = \sqrt{\frac{\hbar D(\mathbf{r})}{2\pi k T}}. \qquad (19)$$

Since these are free parameters, the BCS coherence lengths are determined by the fit procedure. On the other hand, the Ginzburg-Landau coherence length is a function of the magnetic field, see Eq. (14). Since the latter is dictated by the

TABLE I. Fixed material parameters for V, Ag, Nb, and Cu.

	V	Ag	Nb	Cu
$N_{(bulk)}(10^{47}/Jm^3)$	4.50	1.00	12.0	1.98
$T_{c(bulk)}(K)$	4.24	0	8.91	0
$\Theta_D(K)$	390	215	275	315
$v_F(10^8 cm/s)$	0.373	1.39	0.273	1.57

experimental data, ξ is a fixed parameter. But ξ is just the length scale that controls the position of the dimensional crossover, as was discussed in the previous section. To open up the possibility of a real modification of the phase diagram, the value of ξ needs to be changed. Its value has to be uncoupled from the absolute magnitude of the critical fields. Otherwise, the theory does not allow for a simultaneous fit of both the shape and the magnitude of the critical field.

By examining Eq. (4) and realizing that the vector potential $\mathbf{A}$ is proportional to the magnetic field H, it is seen that the only way the field enters into the theory is via the coherence length ξ. Consequently, ξ can be completely uncoupled from the absolute magnitude of H by introducing an extra free parameter into Eq. (14). In the calculations below we will replace this equation by

$$\xi = \sqrt{\frac{\alpha \hbar c}{2eH}}, \qquad (20)$$

while leaving all other equations in which ξ features unchanged. The scaling factor α can be chosen such that ξ matches the typical length scale that controls the experimental dimensional crossover. It may be different for different combinations of metals and layer thicknesses. Thus, the first- and second-solution results will be reconsidered extensively. We are aware that the introduction of the scaling factor lacks a clear physical interpretation. Nevertheless, it will come out that Eq. (20) makes it possible to obtain much better phase diagrams than calculated previously.

V. RESULTS FOR V/Ag

Apart from the scaling of ξ, the fit procedure used to obtain the present results is identical to the one used previously. The fixed material parameters are given by Table I. In applying the fit procedure, we again have a first and a second solution. Both will be considered in the present analysis. In contrast to what was argued for the unscaled results, the second solution now yields the best phase diagrams.

Consider the V(240 Å)/Ag(480 Å) multilayer, of which the unscaled first solution is plotted in Fig. 4 of Ref. 9. The desired achievement of scaling would be that the dimensional crossover shifts to the left. In Fig. 2 this has been accomplished by using a scaling factor $\alpha = 5$. To understand the direction of the shift, consider the role of the Ginzburg-Landau coherence length ξ. At the critical temperature $H_{c2,\parallel}$ vanishes, so according to Eq. (14) the coherence length is infinite. When the temperature decreases, $H_{c2,\parallel}$ increases and, according to the same equation, ξ decreases monotonically. When ξ has become of the same order of magnitude as the layer thicknesses, the dimensional crossover occurs. Let T^* be the temperature at which the second derivative of
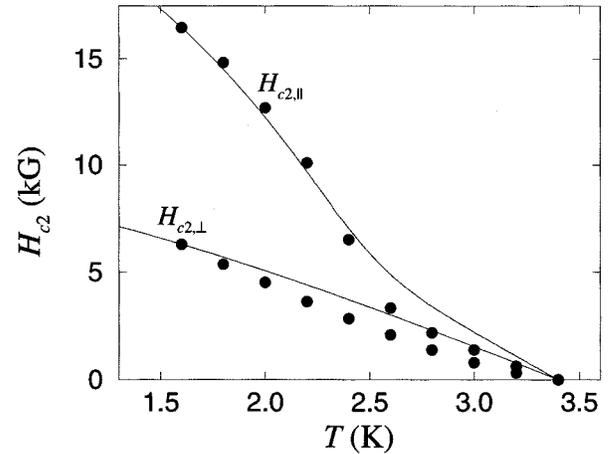
FIG. 2. Upper critical field curve of V(240 Å)/Ag(480 Å). The first solution is shown. A scaling factor $\alpha = 5$ has been employed in the fit procedure. The solid circles show the data points of Kanoda et al. (Ref. 6).

$H_{c2,\parallel}$ is maximum. In Fig. 4 of Ref. 9 this happens at $T^* = 3.32$ K, much earlier than in the experiment. At that temperature the value of $H_{c2,\parallel}$ is 0.97 kG and $\xi = 582$ Å. In calculating Fig. 2, the theory operates at an overall larger coherence length, because of the scaling factor. As a consequence, the dimensional crossover is postponed to $T^* = 2.52$ K. This corresponds to an upper critical field of 5.66 kG and a coherence length $\xi = 539$ Å. Clearly, Fig. 2 considerably improves upon the previous results. T^* is now found at the correct position in the phase diagram. But there are still discrepancies. The scaling factor has had a negligible effect on $H_{c2,\perp}$ and the theory still does not reproduce the experimentally observed positive curvature. Furthermore, $H_{c2,\parallel}$ does not bend as deep as the experiment. The value of α has been chosen such as to produce the most pronounced concavity. For a further increase of α, $H_{c2,\parallel}(T)$ starts tending towards a straight line, since then the three-dimensional regime gradually seizes the temperature domain. So a larger value of α does not mean a further improvement.

The fitting material parameters are $T_{c,V} = 7.79$ K, $D_V = 11.7$ cm²/s, and $D_{Ag} = 20.6$ cm²/s. The value of $T_{c,V}$ is unphysically high for this fit. The ratio of the diffusion coefficients has not changed much compared to the unscaled result. The fact that, via equations like Eq. (13), their average value is related to the magnitude of $1/\xi^2$ is reflected by the fact that both diffusion coefficients have increased by approximately the scaling factor α.

Now consider the second solution, as plotted in Fig. 1. It has a kink at 2.38 K. Compared to the measurements, $H_{c2,\parallel}$ bends too deep and a better result is expected after shifting the kink to the right. Therefore, a scaling factor less than unity has to be adopted. Figure 3 shows the second solution for $\alpha = 0.5$. This curve turns out to fit the data almost perfectly. The discontinuous dimensional crossover in $H_{c2,\parallel}$ has shifted to 3.18 K and is hardly observable any more. It is found that $T^* = 2.95$ K, which is in harmony with the experiment. The perpendicular upper critical field has a positive curvature that is only slightly less than observed in Kanoda's measurements. Clearly, for $\alpha = 0.5$, the coherence lengths have the right magnitude and produce the correct
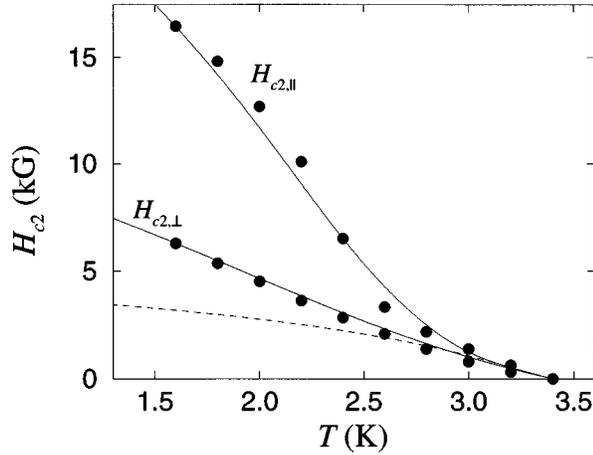
FIG. 3. Upper critical field curve of V(240 Å)/Ag(480 Å). The second solution is shown. A scaling factor $\alpha = 0.5$ has been employed in the fit procedure. The solid circles show the data points of Kanoda *et al.* (Ref. 6).

FIG. 4. Upper critical field curve of Nb(168 Å)/Cu(147 Å). The second solution is shown. A scaling factor $\alpha = 0.333$ has been employed in the fit procedure. The solid circles show the data points of Chun *et al.* (Ref. 4).

type and position of the dimensional crossover.

The fitting material parameters are $T_{c,V} = 5.39$ K, $D_V = 0.583$ cm^2/s, and $D_{Ag} = 30.2$ cm^2/s. The vanadium critical temperature is only slightly less than the unscaled result. The values of D_V and D_{Ag} have decreased, as is expected for α less than unity, but not by a factor of 2. Most of the impact of the scaling factor goes in a moderation of the relative magnitude of the two diffusion coefficients. Whereas for the unscales result we had $D_{Ag}/D_V = 109$, the scaling procedure has changed this to a value of 52. It was observed for all systems that $\alpha < 1$, applied to the second solution, leads to less extreme diffusion coefficients. In case of V(240 Å)/Ag(480 Å), the moderation of the relative magnitude has been such that the undesirable kink has almost been removed from the figure. On the other hand, the ratio is still large enough to produce the positive curvature of the perpendicular upper critical field.

The effect of magnetic-coherence-length scaling is not equally beneficial for the other two multilayers of the same thickness ratio. For V(200 Å)/Ag(400 Å), the second solution for $\alpha = 0.8$ yields a curve that fits $H_{c2,\perp}$ at all temperatures and $H_{c2,\parallel}$ below 2.18 K. Above this temperature, where $H_{c2,\parallel}$ has a discontinuous dimensional crossover, the curve slightly overestimates the experimental data. In this region it is also distinctly convex, which was not found in the measurements. Nevertheless, the fit is still a considerable improvement upon the previous results. For V(160 Å)/Ag(320 Å), the second solution for $\alpha = 0.6$ produces a curve that fits $H_{c2,\perp}$. At 1.21 K, there is a discontinuous dimensional crossover in $H_{c2,\parallel}$. Above this temperature the experimental data is overestimated again, due to the convexity of calculated curve. The two critical fields cannot be fitted simultaneously, that is, for one value of α.

VI. RESULTS FOR Nb/Cu

Proceeding the same way, it is possible to improve upon the phase diagrams of Nb/Cu as well. The fixed parameters are given in Table I. Figure 4 shows the second solution for Nb(168 Å)/Cu(147 Å) with $\alpha = 0.33$. This value yields the
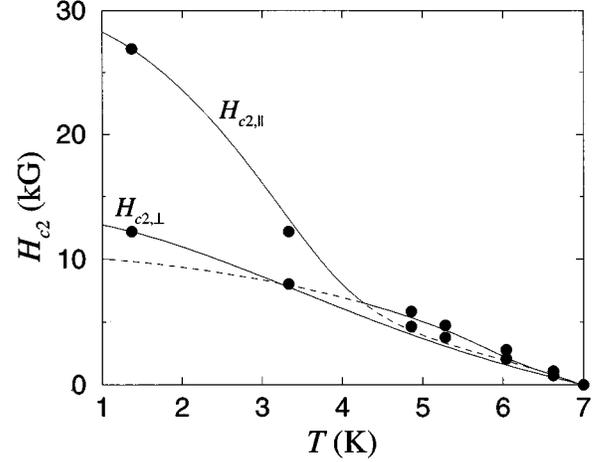
best correspondence to the data of Chun *et al.*[4] The calculated $H_{c2,\parallel}$ curve still exhibits a discontinuous dimensional crossover at 4.27 K. Nevertheless, it reasonably fits the measurements, both above and below the crossover temperature. The $H_{c2,\perp}$ curve is somewhat more concave than the experimental one, but it fits the data much better than the unscaled second solution. The effect of α on the fitting material parameters is that $T_{c,Nb}$ decreases from 9.61 to 9.41 K. D_{Nb} also slightly decreases from 0.58 to 0.51 cm^2/s. The parameter most affected is the diffusion coefficient of copper. D_{Cu} decreases from the extreme value of 231 to a reasonable value of 35 cm^2/s.

Another example is shown in Fig. 5. It is the curve for the Nb(171 Å)/Cu(376 Å) multilayer. The scaling factor employed is $\alpha = 0.25$. It is seen that the data cannot be fitted as good as for the previous system. Near T_c the calculated curve lacks the experimentally observed anisotropy and both $H_{c2,\perp}$ and $H_{c2,\parallel}$ are underestimated. The fitting parameters of
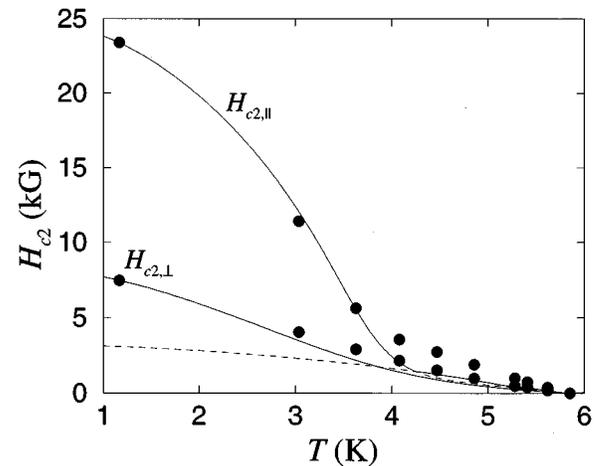
FIG. 5. Upper critical field curve of Nb(171 Å)/Cu(376 Å). The second solution is shown. A scaling factor $\alpha = 0.25$ has been employed in the fit procedure. The solid circles show the data points of Chun *et al.* (Ref. 4).

TABLE II. Fitting parameters for the V/Cu multilayer system.

d_V/d_{Cu} (Å/Å)	T_c (K)	T_{fit} (K)	$T_{c,V}$ (K)	D_V (cm²/s)	D_{Cu} (cm²/s)
250/150	4.55	2.6	7.26	1.49	5.61

this system are $T_{c,Nb}=9.16$ K, $D_{Nb}=0.47$ cm²/s, and $D_{Cu}=104$ cm²/s. The ratio between the diffusion coefficients is still very large, in spite of the scaling factor. However, without scaling, the situation would be even more extreme. In fact, for this system the unscaled fit could not be obtained due to this behavior.

VII. RESULTS FOR V/Cu AND Nb/Ag

According to the position of the elements V, Nb, Ag, and Cu in the Periodic System, V/Ag and Nb/Cu are expected to have similar properties. The analyses given above and in in Ref. 9 show that this expectation holds true. It would of course be interesting to compare these systems to the other two related S/N multilayers: V/Cu and Nb/Ag. A limited number of measurements has been done for these two systems. Dediu et al.[12] published data for V/Cu and Ikebe et al.[13] studied the Nb/Ag system. In both cases only a single phase diagram is shown. Consequently, the analysis cannot be as extensive as it was for the V/Ag and Nb/Cu systems. Nevertheless, it is worthwhile to subject the available data to a fit procedure and compare the fitting parameters to the results of V/Ag and Nb/Cu.

A. Results for the V(250 Å)/Cu(150 Å) system

In analyzing the V(250 Å)/Cu(150 Å) system, N_V, D_V and D_{Cu} were varied in order fit the experimental T_c and $H_{c2,\perp}(T)$ and $H_{c2,\parallel}(T)$ at $T=2.6$ K. Varying N_V is equivalent to varying $T_{c,V}$ at a constant V_V, because these quantities are uniquely related by the BCS expression[14] of the T_c for a bulk superconductor. So we might as well speak of $T_{c,V}$ as the free parameter, which we prefer, as it gives the information in a more appealing way. Apart from $T_{c,V}$, the fixed material parameters of V and Cu are the ones given in Table I. We chose $T_{c(bulk),V}=5.3$ K, the value that is usually reported, instead of the smaller value employed in the analysis of V/Ag. The average value of the Debye temperatures, 303 K, is used.

Table II lists the free parameter values found when applying the fit procedure to the data of Dediu et al.[12] All results correspond to the first solution and no scaling has been applied. It is seen that the fitting vanadium critical temperature is far above the bulk value. It is even comparable to the highest value found in Ref. 9 for V in V/Ag, which was 7.42 K. The vanadium diffusion coefficient falls slightly below the general trend observed in Fig. 2 of Ref. 9. However, considering the scattering in the points, the results are not in contradiction. The copper diffusion coefficient is somewhat higher than the value of 4.93 cm²/s, which is predicted by Eq. (12) of Ref. 9. It falls well in the midst of the results plotted in Fig. 7 of Ref. 9.

Figure 6 shows the calculated phase diagram. The experimental data is represented by the solid circles. The full ex-
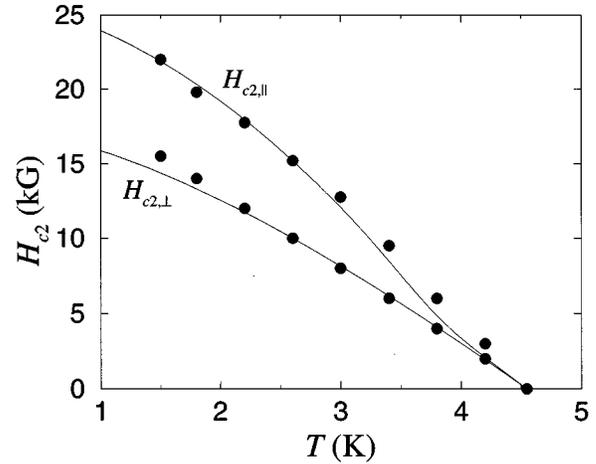
FIG. 6. Upper critical field curve of V(250 Å)/Cu(150 Å). The first solution is shown. The solid circles show the data points of Dediu et al. (Ref. 12).

perimental curve is found in Fig. 2 of Ref. 12. As is seen, both the measured and calculated curves lack a profound dimensional crossover. Consequently, the calculated curve can follow the measured data well. At low temperatures, $H_{c2,\perp}$ is underestimated. Close to the critical temperature, $H_{c2,\parallel}$ is underestimated. It is possible to improve upon Fig. 6 by using a scaling factor for the magnetic coherence length. Figure 7 shows the scaled *second* solution for $\alpha=1.65$. For $H_{c2,\perp}$, the scaled curve lacks the underestimation at low temperatures. Two-dimensional crossovers are observed for $H_{c2,\parallel}$. First, the curve switches continuously from the 3D regime, in which the multilayer behaves as an average bulk metal, to the 2D regime, in which the layered nature of the multilayer starts playing a prominent role. The crossover temperature is $T^*=3.83$ K. The coherence length at T^* is $\xi=257$ Å. Secondly, at $T=1.79$ K the nucleation point shifts discontinuously from Cu to V. At this point the curve exhibits a kink and the coherence length is $\xi=130$ Å. Compared to the unscaled first solution, $H_{c2,\parallel}$ is better able to
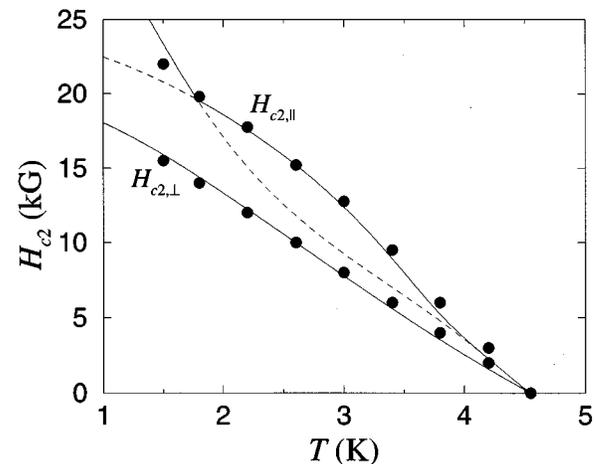
FIG. 7. Upper critical field curve of V(250 Å)/Cu(150 Å). The second solution is shown. A scaling factor $\alpha=1.65$ has been employed in the fit procedure. The solid circles show the data points of Dediu et al. (Ref. 12).

TABLE III. Fitting parameters for the Nb/Ag multilayer system.

d_{Nb}/d_{Ag} (Å/Å)	T_c (K)	T_{fit} (K)	$T_{c,Nb}$ (K)	D_{Nb} (cm^2/s)	D_{Ag} (cm^2/s)
124/124	5.6	1.5	8.15	2.37	3.12

follow the curvature in the measured phase diagram, though at the low-temperature side of the kink it is steeper than desired. It is also possible to use the first solution as the starting point of the scaling procedure. Then an almost linear phase diagram is obtained. It entirely fits $H_{c2,\perp}$ and the linear regimes of $H_{c2,\parallel}$. The factor necessary to achieve this is as large as $\alpha \approx 10$. For such a high value, the dimensional cross-over is completely removed from the picture. It does not show the square-root-like behavior in the central part of the curve.

Dediu et al.[12] observed three distinct regions in their data of $H_{c2,\parallel}$. Below 2.32 and above 3.7 K the curve is linear, which they associated with a three-dimensional behavior of the multilayer. In between the two crossovers a square-root-like temperature dependence is observed, as is characteristic for two-dimensional behavior. At the crossover temperatures there are kinks in $H_{c2,\parallel}(T)$. The crossovers observed by De-diu et al. are qualitatively different from the experimental results for V/Ag. On the one hand, Fig. 2 of Dediu et al. suggests that the multilayer is in the three-dimensional regime over the whole temperature range and that the dent in the curve is caused by some extrinsic effect. The fact that the two linear regimes are in a direct line supports this supposition. On the other hand, it seems improbable that for layers of such thickness there is no intrinsic dimensional crossover. It might well be true that the square-root-like region in $H_{c2,\parallel}(T)$ indeed corresponds to nucleation in copper. That is suggested in Fig. 7, but this figure is not decisive in that respect.

The value of α in Fig. 7 is chosen such that the temperature at which the nucleation point shifts coincides with the leftmost kink of the measurements. For this choice, the low-temperature behavior cannot be reproduced satisfactory. It is remarkable that a factor larger than one has been used to improve upon the unscaled results. An $\alpha < 1$ has the effect of confining the region where nucleation occurs in the normal metal. For V/Ag and Nb/Cu this led to a better agreement with the data. For V/Cu, it is the other way around. By setting $\alpha = 1.65$, we have created a larger region of nucleation in the Cu layer.

B. Results for the Nb(124 Å)/Ag(124 Å) system

For Ag, the fixed material parameters are given in Table I. The parameters chosen for Nb are somewhat different. Now, the more conventional value of $T_{c,Nb(bulk)}$ is used, that is, 9.25 K. The average value of the Debye temperatures is used. It is assumed that V_{Nb}, V_{Ag}, and N_{Ag} are layer-thickness independent. We take $V_{Ag} = 0$, whereas V_{Nb} is calculated from $T_{c,Nb(bulk)}$ and $N_{Nb(bulk)}$. The free parameters are once more N_{Nb}, D_{Nb}, and D_{Ag}, where the value of N_{Nb} will be reported in terms of the corresponding value of $T_{c,Nb}$.
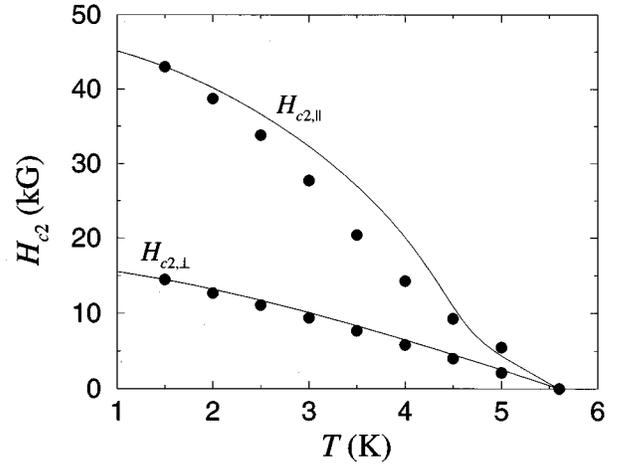
FIG. 8. Upper critical field curve of Nb(124 Å)/Ag(124 Å). The first solution is shown. The solid circles show the data points of Ikebe et al. (Ref. 13).

Using the data of Ikebe et al.[13] and fitting T_c and $H_{c2,\perp}(T)$ and $H_{c2,\parallel}(T)$ at $T = 1.5$ K, the results of Table III are found. We chose the first solution. For all parameters, the fitting values are in reasonable agreement with the results of Ref. 9. The niobium T_c is below the bulk value of 9.26 K, which is in accordance with the behavior of thin films. This is in contrast with the earlier analysis of the much more extensively investigated Nb/Cu system, in which the fitted T_c exceeds bulk T_c. The value found for D_{Nb} is close to the prediction of Eq. (12) of Ref. 9, which is 2.68 cm^2/s. The silver diffusion coefficient is about 2 cm^2/s below the general tendency of D_{Ag} found in V/Ag, as was shown in Fig. 3 of Ref. 9. However, this difference may well be attributed to an actual difference in the purity of the samples used in the experiments.

Figure 8 shows the resulting phase diagram for the Nb(124 Å)/Ag(124 Å) system. The dimensional crossover in the parallel upper critical field is not well reproduced. Its position in the calculated curve is not far off from what is measured, but the curvature below the crossover temperature is larger than what is experimentally observed. Scaled first solutions could only be obtained for scaling factors very close to unity and did not lead to a significant improvement of critical-field curves. Due to an extreme behavior of the diffusion coefficients, scaled and unscaled second solutions cannot be found for this system.

VIII. CONCLUSIONS

The conventional relation between the magnetic field H_{c2} and the magnetic coherence length ξ leads to a wrong mutual dependence of the absolute magnitude of the upper critical fields and the crossover temperature. This can only be overcome by uncoupling H_{c2} and ξ in some way or other. To achieve this, we introduced the concept of magnetic-coherence-length scaling. We conserved the form of the relation between the magnetic field and the coherence length, Eq. (20), but we added a constant scaling factor α that allowed us to control the overall magnitude of ξ independently of H_{c2}. This turned out to open up the possibility of obtaining much better phase diagrams for many of the thick-layer systems. In this context the appreciation for the two solutions of the fit procedure has changed. While in the unscaled ap-

proach the first solution[9] was the preferred one, now the second solution[10] regained its usefulness. For certain multilayer systems, it did a better job than the first solution. However, a satisfactory fit could not be obtained for all systems. Since magnetic-coherence-length scaling lacks an external justification, the fact that it works is an indication that the Takahashi-Tachiki theory needs a modification in order to give a realistic quantitative description of upper critical fields of real metallic multilayers.

Previous publications[9,10] only concerned V/Ag and Nb/Cu. In this paper, the discussion was extended to two additional combinations of metals into multilayers: V/Cu and Nb/Ag. However, for these systems, the limited amount of experimental data did not allow for an equally extensive analysis. The fitting material parameters for the first solution could well be reconciled with the findings for the two related systems V/Ag and Nb/Cu. For vanadium, the T_c found was high, but inside the range of values found for V in V/Ag. The

niobium T_c, on the other hand, was below the bulk niobium value, but again inside the range of values found for Nb in Nb/Cu. Compared to the earlier results, reasonable values were obtained for the fitting diffusion coefficients. The experimental phase diagram of V/Cu was somewhat dissimilar to the diagrams found for the related systems. The difference suggested the existence of a temperature domain in which superconductivity nucleates in the middle of the Cu layer.

ACKNOWLEDGMENTS

[1] I. Banerjee, Q. S. Yang, C. M. Falco, and I. K. Schuller, Solid State Commun. **41**, 805 (1982).

[2] I. Banerjee, Q. S. Yang, C. M. Falco, and I. K. Schuller, Phys. Rev. B **28**, 5037 (1983).

[3] I. Banerjee and I. K. Schuller, J. Low Temp. Phys. **54**, 501 (1984).

[4] C. S. Chun, G-G. Zheng, J. L. Vicent, and I. K. Schuller, Phys. Rev. B **29**, 4915 (1984).

[5] K. Kanoda, H. Mazaki, T. Yamada, N. Hosoito, and T. Shinjo, Phys. Rev. B **33**, 2052 (1986).

[6] K. Kanoda, H. Mazaki, N. Hosoito, and T. Shinjo, Phys. Rev. B **35**, 6736 (1987).

[7] P. R. Broussard and T. H. Geballe, Phys. Rev. B **35**, 1664 (1987).

[8] P. R. Broussard and T. H. Geballe, Phys. Rev. B **37**, 60 (1988).

[9] R. T. W. Koperdraad and A. Lodder, Phys. Rev. B **51**, 9026 (1995).

[10] R. T. W. Koperdraad and A. Lodder, Proc. SPIE **2157**, 252 (1994).

[11] S. Takahashi and M. Tachiki, Phys. Rev. B **33**, 4620 (1986).

[12] V. I. Dediu, V. V. Kabanov, and A. S. Sidorenko, Phys. Rev B **49**, 4027 (1994).

[13] M. Ikebe, Y. Obi, Y. Kamiguchi, Y. Fukumoto, H. Nakajima, Y. Muto, and H. Fujimori, Jpn. J. Appl. Phys. **26**, 1997 (1987).

[14] The various formulations and approximations in which the theory appears have been summarized and compared by A. Lodder and R. T. W. Koperdraad, Physica C **212**, 81 (1993).

[15] L. P. Gorkov, Sov. Phys. JETP **10**, 998 (1960).

[16] P. R. Auvil, J. B. Ketterson, and S. N. Song, J. Low Temp. Phys. **74**, 103 (1989).

[17] P. G. de Gennes, Rev. Mod. Phys. **36**, 225 (1964).